Scattering of $\bar{H}(1s)$ off metastable helium atom at thermal energies

Prabal K. Sinha
Department of Physics, Bangabasi College, 19, Raj Kumar Chakravorty Sarani, Kolkata 700 009, India

A. S. Ghosh*
Department of Theoretical Physics, Indian Association for the Cultivation of Science, Jadavpur, Kolkata 700 032, India
(Received 24 October 2005; published 12 June 2006)

Quantal calculations for scattering of ground-state antihydrogen by metastable ($n=2S$) helium atoms have been performed using the nonadiabatic, atomic orbital expansion technique at thermal energies. The zero-energy elastic cross sections of the present systems are much greater than the corresponding value for the ground-state helium target. The low-energy elastic cross section for the singlet metastable helium [He($2\,^1S$)] target is higher than the corresponding value when the target is in the metastable triplet state [He($2\,^3S$)].

DOI: 10.1103/PhysRevA.73.062710 PACS number(s): 34.90.+q, 36.10.−k, 31.15.Ar, 32.80.Pj

I. INTRODUCTION

The last few years have witnessed a tremendous development in experimental techniques for the production of the antihydrogen atom ($\bar{H}$) at cryogenic temperatures [1–6]. A few properties of the antiatom have also been investigated through actual experimentation. The early production of $\bar{H}$ at CERN [1] and Fermi Lab [2] has stimulated theoretical studies of $\bar{H}$ interacting with normal atoms at ultracold temperatures. Up to now a good few attempts have been made to estimate different scattering probabilities for $\bar{H}$-H system at low incident energies using adiabatic [7,8] and nonadiabatic [9] calculation techniques. The above theoretical studies may be summarized as follows: in consideration of the same physical effects, the adiabatic and nonadiabatic calculations yield almost the same values for the *s*-wave elastic scattering parameters for the $\bar{H}$-H system at thermal energies; rearrangement processes have a marginal effect on the elastic scattering although there is ambiguity about the values of the rearrangement cross sections; the effect of the strong interaction is found to increase the elastic cross section to some extent for an atomic hydrogen target [7,8,10]. Studies on the interaction of the $\bar{H}$-He system have also begin to appear in the literature [11–15]. For a ground-state He target, the strong interaction has been reported to have considerable effect on the elastic channel [14] for the system. Sinha and Ghosh have performed nonadiabatic calculations for the *s*-wave elastic scattering of $\bar{H}$ off an atomic lithium target [16] at low energies. The high values of the elastic cross section for this system suggest that Li($2s$) may be a more efficient buffer gas, compared to ground-state H and He, in cooling $\bar{H}$ to ultracold temperatures. We have also investigated the *s*-wave elastic scattering of antihydrogen atom off atomic metal targets (Li to Rb) [17]. The leptonic potential energy for the systems are expected to be free from any barrier or hump.

From the academic point of view, investigations of $\bar{H}$ scattering off different atomic and molecular targets are of importance as such studies will explore the interaction dynamics which are very little known to date. On the other hand, from the experimental point of view $\bar{H}$-He and $\bar{H}$-H_2 systems will provide information about the cooling of antiatoms in different (He and H_2) buffer gases. Information about the elastic and inelastic cross sections of $\bar{H}$ with different atomic and molecular gas targets will be helpful in proper design of experiments for effective cooling of exotic atomic samples.

The investigation of atomic scattering processes involving metastable atomic targets is always a fascinating field of study as the metastable atoms have high dipole polarizability and low excitation and ionization thresholds compared to the corresponding values of the stable state. On the other hand, the metastable atoms have lifetimes large enough to allow for scattering experiments. For a scattering calculation involving metastable atoms the lowest-order long-range interactions, R^{-4} for ion impact scattering and R^{-6} for atom impact scattering, are expected to dominate the scattering dynamics which results in a high value for the elastic cross section. The metastable states of rare-gas atoms have special features; in addition to the properties of other metastable atoms, they have large core excitation energy and high cross sections (this has been confirmed theoretically [18] as well as experimentally [19] for electron impact scattering). From the theoretical point of view, the investigation of ground-state antihydrogen [$\bar{H}(1s)$] interacting with metastable helium atoms [He($2\,^1S$)] or [He($2\,^3S$)] is of prime interest. A recent calculation [15] has reported the adiabatic leptonic potential energy curve for the $\bar{H}(1s)$+He($2\,^3S$) system and estimated semiclassically the rearrangement cross section. The adiabatic potential energy curve reported for the system does not show either a barrier or a hump. Such an interaction is a characteristic of $\bar{H}$+alkali metal systems rather than antihydrogen–noble gas interactions. It is worth mentioning that the lowest triplet state of helium, viz., He($2\,^3S$), has a variety of experimental applications, ranging from its relevance to Bose-Einstein condensation [20] and to the study of surface magnetism [21]. On the other hand, the singlet metastable state of helium, viz., He($2\,^1S$), has application in diagnosing the internal electric field of a Penning plasma

*Email address: tpasg@mahendra.iacs.res.in

[22]. Furthermore, recent experimental techniques are capable of producing both metastable states at ultracold temperatures.

The peculiarities of metastable helium states and the experimental need for better design of experiments to cool $\bar{H}$ have motivated us to undertake a theoretical calculation for the scattering of the ground-state antihydrogen atom off these metastable species at low incident energies where the quantum effects are important. We have chosen the theoretical model in such a way that due attention has been paid to the long-range forces. Such a study will reveal the dynamics of antihydrogen interaction with metastable helium species. Furthermore, if a chamber contains some charged particles in addition to buffer gases (He and H_2) the charged particle will execute Landau trajectories under the action of the trapping magnetic field. Due to the repeated collisions of charged particles with the ground-state helium atom, some of the atoms [23] will be excited to metastable states, which in turn may interact with the antiatom. It has been argued [19] that the presence of a small fraction of metastable helium may change the discharge phenomena appreciably due to the high collision cross section of electron off metastable helium. Such a phenomenon is not very unlikely in a gas chamber containing charged particles, especially electrons, provided that the metastable helium has a large cross section compared to that of ground-state helium for antihydrogen impact scattering.

II. THEORY

For the sake of completeness of the present paper, here we present a description of our theoretical model. The bound state of the target (He) atom with wave functions $\phi_\eta(\vec{r}_1,\vec{r}_2)$ is described by the time-independent Schrödinger equation:

$$H_{\mathrm{He}}\phi_\eta(\vec{r}_1,\vec{r}_2)=\epsilon_\eta^{\mathrm{He}}\phi_\eta(\vec{r}_1,\vec{r}_2) \tag{1}$$

where $\vec{r}_1$ and $\vec{r}_2$ are the positions of the two electrons with respect to the center of mass of the He atom and the Hamiltonian is given by

$$H_{\mathrm{He}}=-\frac{1}{2}\nabla_1^2-\frac{1}{2}\nabla_2^2-\frac{Z}{r_1}-\frac{Z}{r_2}+\frac{1}{|\vec{r}_1-\vec{r}_2|}. \tag{2}$$

To describe the bound-state wave functions of the helium atom we used the orbitals due to Winter and Lin [24]. The state of a He atom in which one of the electrons lies in the ground state $(1s)$ while the other is in any arbitrary state $(nlm$, excluding $1s)$ is written as

$$\phi_{n^SLM}(\vec{r}_1,\vec{r}_2)=\frac{N_{n^SL}}{\sqrt{2}}[p(r_1)v_{n^SLM}(\vec{r}_2)\pm p(r_2)v_{n^SLM}(\vec{r}_1)] \tag{3}$$

where $p(r)=\sqrt{Z^3/\pi}e^{-Zr}$ is the normalized ground-state wave function of the helium ion (He^+) with $Z=2$ and

$$v_{n^SLM}(\vec{r})=r^L Y_{LM}(\hat{r})e^{-\alpha(n^SL)r}\sum_{k=1}^{n-L}(-1)^{k-1}c(n^SL,k)r^{k-1}. \tag{4}$$

The optimized values for the range parameter (α), expansion coefficient (c), and normalization constant (N) are provided by the authors of [24] together with the eigenenergies for states up to $4\,{}^SD$, where the multiplicity $S=1$ for helium electrons having antiparallel spin alignments (singlet) and $S=3$ for parallel spins (triplet). The total wave functions ϕ form an orthonormal basis set for the He atom. This wave function treats both the electrons on equal footing and allows the exchange of electrons of the He atom. It is to be noted that the singlet states (ground and excited) of He have been employed by us [12,13] for the ground-state target. Our s-wave elastic scattering length without strong interaction was confirmed later [14].

The bound-state wave functions $\bar{\phi}_\nu(\vec{r}_p)$ of the projectile atom are determined by the equation

$$H_{\bar{\mathrm{H}}}\bar{\phi}_\nu(\vec{r}_p)=\epsilon_\nu^{\bar{\mathrm{H}}}\bar{\phi}_\nu(\vec{r}_p) \tag{5}$$

where $\vec{r}_p$ is the position vector of the positron measured from the antiproton, the center of mass of the antiatom. The Hamiltonian of the projectile atom is

$$H_{\bar{\mathrm{H}}}=-\frac{1}{2}\nabla_{r_p}^2-\frac{1}{r_p}. \tag{6}$$

The total Hamiltonian of this interaction system is given by

$$H=H_{\mathrm{He}}+H_{\bar{\mathrm{H}}}-\frac{1}{2\mu}\nabla_R^2+V_{int}. \tag{7}$$

The separation between the centers of mass of the colliding atoms is represented by $\vec{R}$. The third term on the right-hand side of the above equation represents the relative kinetic energy between the centers of mass of the system, while the last term is the interaction potential and is given by

$$V_{int}=-\frac{Z}{R}+\frac{Z}{|\vec{R}+\vec{r}_p|}-\frac{1}{|\vec{R}+\vec{r}_p-\vec{r}_1|}-\frac{1}{|\vec{R}+\vec{r}_p-\vec{r}_2|}+\frac{1}{|\vec{R}-\vec{r}_1|}+\frac{1}{|\vec{R}-\vec{r}_2|}. \tag{8}$$

The theory of the close-coupling approximation (CCA) is based on the expansion of the total wave function $\psi(\vec{r}_1,\vec{r}_2,\vec{r}_p,\vec{R})$ in terms of wave functions $\bar{\phi}_\nu(\vec{r}_p)$ and $\phi_\eta(\vec{r}_1,\vec{r}_2)$ describing the bound states of $\bar{H}$ and He atoms:

$$\psi(\vec{r}_1,\vec{r}_2,\vec{r}_p,\vec{R})=\sum_{\nu,\eta}\bar{\phi}_\nu(\vec{r}_p)\phi_\eta(\vec{r}_1,\vec{r}_2)F_{\nu,\eta}(\vec{R}), \tag{9}$$

where $F_{\nu,\eta}(\vec{R})$ represents the scattering function with the usual asymptotic boundary conditions. The three-dimensional coupled equation for the unknown scattering amplitude in momentum space, $f_{\nu'\eta';\nu\eta}(\vec{k}',\vec{k})$, for the transition $\bar{\mathrm{H}}_\nu+\mathrm{He}_\eta\rightarrow\bar{\mathrm{H}}_{\nu'}+\mathrm{He}_{\eta'}$, is given by

$$f_{\nu'\eta';\nu\eta}(\vec{k}',\vec{k})=f^{B}_{\nu'\eta';\nu\eta}(\vec{k}',\vec{k})-\frac{1}{2\pi^2}\times\sum_{\nu''\eta''}\int d\vec{k}''\frac{f^{B}_{\nu'\eta';\nu''\eta''}(\vec{k}',\vec{k}'')f_{\nu''\eta'';\nu\eta}(\vec{k}'',\vec{k})}{k^2_{\nu''\eta''}-k''^2+i\epsilon}. \tag{10}$$

Here ν and η denote, respectively, the sets of quantum numbers nlm of the projectile and the target (one-electron excitation) atoms. The first-order (Born) scattering amplitude is denoted by f^B and is given by

$$f^B_{\nu'\eta';\nu\eta}(\vec{k}',\vec{k}) = -\frac{\mu}{2\pi}\int \bar{\phi}^*_{\nu'}(\vec{r}_p)\phi^*_{\eta'}(\vec{r}_1,\vec{r}_2)e^{-\vec{k}'\cdot\vec{R}}V_{int} \times \bar{\phi}_{\nu}(\vec{r}_p)\phi_{\eta}(\vec{r}_1,\vec{r}_2)e^{\vec{k}\cdot\vec{R}}d\vec{R}\,d\vec{r}_p d\vec{r}_1 d\vec{r}_2 \quad (11)$$

where $\vec{k}$ and $\vec{k}'$ are the momenta in the initial and the final channels, respectively, and are related to the eigenenergies as

$$\frac{k^2}{2\mu} + \epsilon^{\bar{\mathrm{H}}}_{\nu} + \epsilon^{\mathrm{He}}_{\eta} = \frac{k'^2}{2\mu} + \epsilon^{\bar{\mathrm{H}}}_{\nu'} + \epsilon^{\mathrm{He}}_{\eta'}. \quad (12)$$

$\frac{1}{\mu} = \frac{1}{M_{\mathrm{H}}} + \frac{1}{M_{\mathrm{He}}}$ is the reduced mass of the system and $\vec{Q} = \vec{k} - \vec{k}'$ is the momentum transfer. On performing the integration over $\vec{R}$, using the Bethe formula, the first-order amplitude for direct scattering decouples into the projectile and target factors:

$$f^B_{\nu'\eta';\nu\eta}(\vec{k}',\vec{k}) = \frac{2\mu}{Q^2} I^{\mathrm{He}}_{\eta';\eta}(\vec{Q}) \times I^{\bar{\mathrm{H}}}_{\nu';\nu}(\vec{Q}) \quad (13)$$

where

$$I^{\mathrm{He}}_{\eta';\eta}(\vec{Q}) = \int \phi^*_{\eta'}(\vec{r}_1,\vec{r}_2)(Z - e^{i\vec{Q}\cdot\vec{r}_1} - e^{i\vec{Q}\cdot\vec{r}_2})\phi_{\eta}(\vec{r}_1,\vec{r}_2)d\vec{r}_1 d\vec{r}_2 \quad (14)$$

and

$$I^{\bar{\mathrm{H}}}_{\nu';\nu}(\vec{Q}) = \int \bar{\phi}^*_{\nu'}(\vec{r}_p)(1 - e^{-i\vec{Q}\cdot\vec{r}_p})\bar{\phi}_{\nu}(\vec{r}_p)d\vec{r}_p. \quad (15)$$

In partial wave analysis one expands the scattering amplitudes (f or f^B) in terms of the spherical harmonics as [13]

$$f_{\nu'\eta';\nu\eta}(\vec{k}',\vec{k}) = \frac{1}{\sqrt{kk'}}\sum_{JM}\sum_{J_1M_1}\sum_{J'_1M'_1}\sum_{LM_L}\sum_{L'M'_L} \times \begin{pmatrix} L' & l'_p & J'_1 \\ M'_L & m'_p & M'_1 \end{pmatrix}\begin{pmatrix} J'_1 & l'_t & J \\ M'_1 & m'_t & M \end{pmatrix} \times Y^*_{L'M'_L}(\hat{k}')T^J(\tau'k';\tau k)Y_{LM_L}(\hat{k}) \times \begin{pmatrix} L & l_p & J_1 \\ M_L & m_p & M_1 \end{pmatrix}\begin{pmatrix} J_1 & l_t & J \\ M_1 & m_t & M \end{pmatrix} \quad (16)$$

and a similar expression for f^B with T^J on the right side replaced by B^J. Here l_p and l_t are the angular momenta of the bound projectile and the target atoms, respectively, and J is the total angular momentum of the colliding system, which comprises three angular momenta l_p, l_t, and L. τ represents the set of quantum numbers (n_p,l_p,n_t,L_t,J_1,L). On simplification, Eq. (10) becomes a one-dimensional coupled equation for unknown amplitudes T^J as

$$T^J(\tau'k';\tau k) = B^J(\tau'k';\tau k) - \frac{1}{2\pi^2}\sum_{\tau''}\int dk''k''\frac{B^J(\tau'k';\tau''k'')T^J(\tau''k'';\tau k)}{k^2_{\nu''\eta''} - k''^2 + i\epsilon}. \quad (17)$$

To solve these equation one needs B^J's as input. With a knowledge of f^B [from Eq. (13)] one can get, by inverting Eq. (16),

$$B^J(\tau'k';\tau k) = \frac{\sqrt{kk'}}{(2J+1)}\sum_{MM_LM'_L}\sum_{m_am'_a}\sum_{m_pm'_p} \times \begin{pmatrix} L' & l'_p & J'_1 \\ M'_L & m'_p & M'_1 \end{pmatrix}\begin{pmatrix} J'_1 & l'_t & J \\ M'_1 & m'_t & M \end{pmatrix} \times \begin{pmatrix} L & l_p & J_1 \\ M_L & m_p & M_1 \end{pmatrix}\begin{pmatrix} J_1 & l_t & J \\ M_1 & m_t & M \end{pmatrix} \times \int d\hat{k}\int d\hat{k}' Y^*_{L'M'_L}(\hat{k}')f^B_{\nu'\eta';\nu\eta}(\vec{k}',\vec{k})Y_{LM_L}(\hat{k}). \quad (18)$$

Once Eq. (17) is solved, all the necessary information about the scattering parameters can easily be obtained. For the Jth partial wave scattering at incident momentum k_0, the real part of the elastic phase shift is given as

$$\delta_J(k_0) = \frac{1}{2}\tan^{-1}\left(\frac{\mathrm{Re}[T^J(\tau_0k_0;\tau_0k_0)]}{2\pi - \mathrm{Im}[T^J(\tau_0k_0;\tau_0k_0)]}\right) \quad (19)$$

where $\tau_0 = (1,0,2,0,J,J)$ designates the initialization of the system and the cross section for a transition $\bar{\mathrm{H}}(1s) + \mathrm{He}(n_tS) \rightarrow \bar{\mathrm{H}}(n'_pl'_p) + \mathrm{He}(n'_tL'_t)$ is given by

$$\sigma_J(k_0) = \sum_{L'J'_1}\frac{(2J+1)}{4\pi k_0^2}|T^J(\tau'k';\tau_0k_0)|^2. \quad (20)$$

III. MODELS

To investigate the elastic scattering of the ground-state antihydrogen atom $[\bar{\mathrm{H}}(1s)]$ off atomic metastable helium in singlet $[\mathrm{He}(2\,^1S)]$ and triplet $[\mathrm{He}(2\,^3S)]$ states we employ the close-coupling approximation. This model is *ab initio* and nonadiabatic in nature. The effect of different physical features can be accounted for in the calculation dynamically by suitable choice of the basis set. The accuracy of the predicted results certainly depends on the judicial choice of the expansion basis. The systems under consideration are known to have high values of dispersion coefficient [25]. As a result the accuracy of any scattering calculation will depend on the extent to which the long-range interactions are incorporated in the calculation. In a CCA calculation the van der Waals interaction, which arises from the interaction of the induced dipoles of the colliding atoms, can be taken into consideration by retaining the p states of the interacting atoms. The coverage of this attractive effect depends on how much of the induced dipole polarizability of the atoms is accounted

for by the atomic orbitals used to generate the basis set. The other higher-order long-range forces are included in the CCA calculation by retaining still higher-angular-momentum states. Guided by this, we chose the $\bar{\mathrm{H}}$ wave functions in such a way that the majority of dipole and quadrupole polarizabilities of the projectile atom are considered. Literature reveals that the p and d pseudostates of the hydrogen atom, viz., $\mathrm{H}(2\bar{p})$ and $\mathrm{H}(3\bar{d})$, account for these effects fully [26]. To compare the goodness of such a description of the projectile atom we have also used a set of projectile states that contains $n=3$ and 4 pseudostates in addition to $n\leq 2$ eigenstates [27]. Inclusion of $n=3$ and 4 pseudostates also allows us to take into account the effect of the projectile continuum as a whole on the elastic channel. The latter set of pseudostates has been previously found to be suitable in studying the elastic scattering of e^--atom [27], e^+-atom [28], Ps-H [29], and e^--Ps [30] systems. The basis sets used in the present investigations are

$$\bar{\mathrm{H}}(1s,2s,2\bar{p},3\bar{d}) + \mathrm{He}(2\,^S S, 2\,^S P), \quad \text{model A},$$

$$\bar{\mathrm{H}}(1s,2s,2p,3\bar{s},3\bar{p},3\bar{d},4\bar{s},4\bar{p},4\bar{d}) + \mathrm{He}(2\,^S S, 2\,^S P), \quad \text{model B},$$

$$\bar{\mathrm{H}}(1s,2s,2\bar{p},3\bar{d}) + \mathrm{He}(2\,^S S, 2\,^S P, 3\,^S S, 3\,^S P, 3\,^S D), \quad \text{model C},$$

$$\bar{\mathrm{H}}(1s,2s,2\bar{p},3\bar{d}) + \mathrm{He}(2\,^S S, 2\,^S P, 3\,^S S, 3\,^S P, 3\,^S D, 4\,^S S, 4\,^S P, 4\,^S D), \quad \text{model D}.$$

All the four models listed above contain pseudostates of the projectile atom; consequently, such CCA models are termed pseudostate close-coupling approximations (PSCCAs). One of the main advantages of the CCA model is that one does not need to calculate the leptonic potential for the system separately. A sufficiently good description of the isolated atomic states is sufficient for the dynamic generation of the potentials (both short and long range) of interest.

The two-body dispersion coefficients for the interaction of two atoms A and B are given by $C_{2n}^{AB}=(2n-2)!\sum_{l=1}^{n-2}\frac{1}{2\pi(2l)!(2n-2l-2)!}\int_0^\infty \alpha_l^A(i\omega)\alpha_{n-l-1}^B(i\omega)d\omega$, where $\alpha_l^A(i\omega)$ is the dynamic polarizability of order l of atom A at the imaginary frequency ω [31]. The values of the dispersion coefficients accounted for in the CCA calculations can be obtained by solving the Schrödinger equation for the system. To have an idea about the dispersion coefficients, we employ a first-order definition of the atomic polarizabilities [32]. The coefficient C_6, as stated earlier, arises from dipole-dipole interaction, and C_8 from dipole-quadrupole and quadrupole-dipole interactions. The values of the first three dispersion coefficients accounted for in all the four CCA models for both the systems are listed in Table I together with the corresponding standard values [25]. For the triplet target the model D accounts for about 90% of C_6 while for the singlet case a coverage of more than 98% is achieved. The models A and B estimate C_8 rather crudely. This is due to the fact that these two models do not contain any d state of the target atom and consequently the dipole (projectile)–quadrupole (target) contribution to C_8 is absent, whereas the other two models consider C_8 satisfactorily (Table I). However, for the singlet target, model D overestimates this effect by about 3%. The amount of overestimation may be reduced in still higher-order calculations. Our last two models consider only the quadrupole-quadrupole contribution to C_{10}. It is to be noted that the contribution to C_{10} arising from dipole-octopole and octopole-dipole interactions has been totally neglected and as a result the coefficient C_{10} has been underestimated. We argue that the values of C_6 and C_8 accounted for in our CCA calculations are more refined than those listed in Table I and the incorporation of the long-range forces is satisfactory.

TABLE I. Comparison of the dispersion coefficients (in a.u.) $E_{dis}=-C_6/R^6-C_8/R^8-C_{10}/R^{10}$ for the interaction of ground-state hydrogen [H(1s)] with different atomic targets. $A[m]$ means $A\times 10^m$.

System	C_6	C_8	C_{10}
H(1s)+H(1s) [33]	6.499[0]	1.244(2)	3.285(3)
H(1s)+He(1 ^1S) [33]	2.821[0]	4.184(1)	8.715(2)
H(1s)+He(2 ^1S)			
Model A	1.149[2]	9.698[2]	0
Model B	1.149[2]	9.676[2]	0
Model C	1.231[2]	9.652[3]	1.401[5]
Model D	1.254[2]	1.025[4]	1.496[5]
Ref. [25]	1.274[2]	9.903[3]	1.027[6]
H(1s)+He(2 ^3S)			
Model A	7.622[1]	6.499[2]	0
Model B	7.618[1]	6.485[2]	0
Model C	7.718[1]	3.144[3]	4.093[4]
Model D	7.760[1]	3.586[3]	4.820[4]
Ref. [25]	8.654[1]	4.959[3]	3.931[5]
H(1s)+Li(2s) [37]	6.654[1]	3.280[3]	2.230[5]

IV. RESULTS AND DISCUSSION

This paper reports the results for ground-state antihydrogen [$\bar{\mathrm{H}}(1s)$] scattering by the $n=2S$ metastable states of the helium atom. As there is no other result for the systems available, the present results could not be compared. Nonadiabatic pseudostate close-coupling approximations with different basis sets have been employed to get an idea about the convergence of the predicted values with added states in the expansion basis. The s-wave elastic cross sections and phase shifts are presented in the energy range 10^{-16} to 10^{-4} a.u. The highest energy considered here corresponds to a temperature of order of 30 K.

A. Convergence

Tables II and III compare the performances of the different sets of pseudostates used to address the effect of distortion of the projectile atom. The two sets of hydrogenic pseudo-states (models A and B) are found to predict s-wave

TABLE II. Comparison of *s*-wave elastic phase shifts (rad) for $\bar{H}(1s)+He(2\,^3S)$ system using different PSCCA models. $A[m]$ means $A\times 10^m$.

E (a.u.)	Model A	Model B	Model C	Model D
10^{-16}	−0.1054[−4]	−0.1060[−4]	−0.8566[−5]	−0.8407[−5]
10^{-14}	−0.1054[−3]	−0.1060[−3]	−0.8566[−4]	−0.8408[−4]
10^{-12}	−0.1054[−2]	−0.1060[−2]	−0.8568[−3]	−0.8410[−3]
10^{-10}	−0.1056[−1]	−0.1063[−1]	−0.8581[−2]	−0.8422[−2]
10^{-8}	−0.1056[0]	−0.1086[0]	−0.8594[−1]	−0.8436[−1]
10^{-6} [35]	+0.5361[0]	+0.5400[0]	+0.6967[0]	+0.7095(0)
10^{-4}	+0.6635[−1]	+0.7485[−1]	+0.2830[0]	+0.3054(0)

elastic results within an acceptable range of tolerance, for both systems. The effects of the $n=3$ (model C) and 4 (model D) states of He atom on the elastic channels have also been examined (Tables II and III). The results are found to be nearly convergent with the addition of He states in the expansion basis for the triplet metastable target while for the singlet metastable target there is scope for improving the result marginally. It is to be noted that the model D accounts for about 98% of the exact value of C_6 for a singlet target while for triplet target our model D considers 90% of the van der Waals interaction. The discrepancy among between the exact value of c_6 and that accounted for in model D is due to the neglect of the continuum of the target atoms.

The phase shifts of Tables II and III are given in the range $\pm\pi/4$ [34]. Obviously these values will not always reproduce the cross section as is the case for the last two energies tabulated [35]. To avoid this and also to have an idea about the continuous variation of phase shifts with incident momentum ($k=\sqrt{2E/\mu}$), we plot the phase shifts [36] of all the models in the entire energy range. Figure 1 represents the variation of the *s*-wave elastic phase shift for the triplet target, while Fig. 2 depicts the same for the singlet target. The phase shifts for both systems are variationally consistent, i.e., with enlargement of the basis set the interaction potential becomes more attractive, which results in higher values of phase shifts at low energies.

$\bar{H}(1s)+He(2\,^3S)$ system

The results of *s*-wave elastic scattering of ground-state antihydrogen atoms by the lowest triplet metastable He atom is presented in this section. Table II compares the *s*-wave elastic phase shifts [34] for the system as predicted by the different PSCCA models, at a few selected energies covering the range of the present study. In both the models A and B, the target atom is described by the two lowest triplet states, viz., $2\,^3S$ and $2\,^3P$, while the projectile antiatom is described, respectively, by a four-state (two eigen- and two pseudostates) and a nine-state (three eigen- and six pseudostates) basis. The phase shifts (Fig. 1) of models A and B differ marginally over the entire range of energies. This shows that both the sets of atomic orbitals selected for representing the antihydrogen atom are equally good, at least for the thermal energy *s*-wave elastic scattering of the present system. Figure 3 shows that the elastic cross sections of the system obtained by using models A and B are indistinguishable from one another all over the energy range considered in this investigation. At very low energies where the cross section is independent of incident energies, there is a difference of about 1% between the two sets of values for the elastic cross section. In the four-state description of the projectile atom a complete consideration of the atomic distortion via dipole and quadruple moments has been incorporated in the calculation. Apart from this, a part of the continuum effect has been introduced in the calculation. We could argue that both the descriptions of the projectile atom are equivalent. So to save computational labor, which is enormous in atom-atom systems, we have opted for a four-state description of the projectile.

A metastable state is known to have high values of dipole polarizibility compared to its ground-state counterpart (see Table I). Thus, the next natural search should be to find the

TABLE III. Comparison of *s*-wave elastic phase shifts (rad) for the $\bar{H}(1s)+He(2\,^1S)$ system using different PSCCA models. $A[m]$ means $A\times 10^m$.

E (a.u.)	Model A	Model B	Model C	Model D
10^{-16}	−0.3046[−4]	−0.3040[−4]	−0.1976[−4]	−0.1844[−4]
10^{-14}	−0.3047[−3]	−0.3041[−3]	−0.1973[−3]	−0.1844[−3]
10^{-12}	−0.3049[−2]	−0.3043[−2]	−0.1977[−2]	−0.1845[−2]
10^{-10}	−0.3064[−1]	−0.3058[−1]	−0.1988[−1]	−0.1851[−1]
10^{-8}	−0.3028[0]	−0.3023[0]	−0.1938[0]	−0.1845[0]
10^{-6} [35]	−0.3667[0]	−0.3656[0]	−0.5894[−1]	−0.9227[−2]
10^{-4}	+0.5446[0]	+0.5466[0]	+0.7006[0]	+0.7225[0]

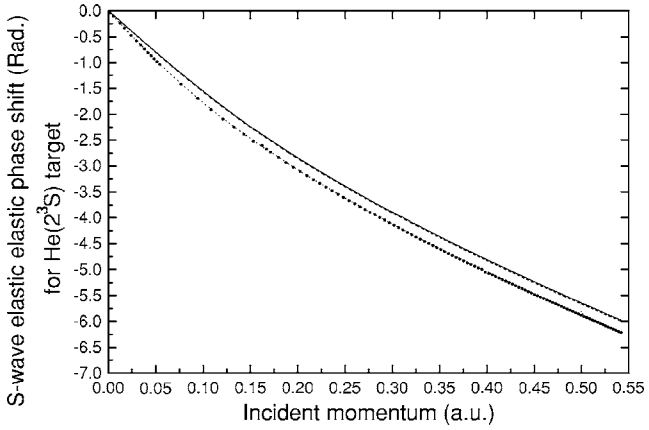

FIG. 1. s-wave elastic phase shift (modulus π) for $\bar{H}(1s)+He(2\,^3S)$ scattering. Curves: circles, model A; dotted, model B; dashed, model C; solid, model D.

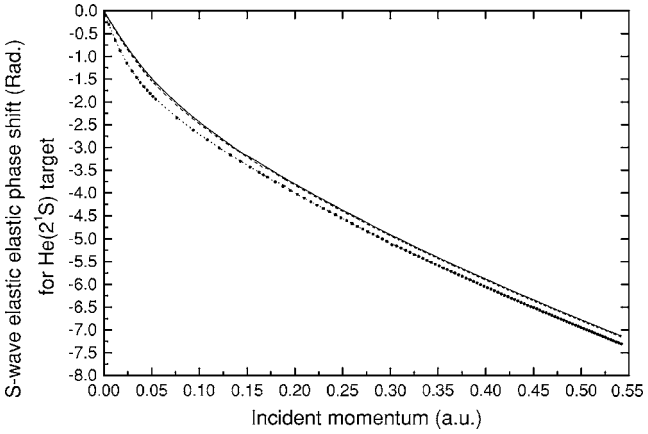

FIG. 2. s-wave elastic phase shift (modulus π) for $\bar{H}(1s)+He(2\,^1S)$ scattering. Curves: circles, model A; dotted, model B; dashed, model C; solid, model D.

convergence of the predicted results with the addition of still higher states of the metastable atom. To this end, in model C, we have included the $n=3$ single-excitation triplet states of the He atom. The $n=3$ states of the He atom are found to have an appreciable effect on the elastic scattering, as is evident from Table II and Fig. 3. The zero-energy cross section of model C decreases by about 34% from the corresponding value of model A. Since the values for the scattering parameters predominantly depend on the long-range behavior of the interaction potential, this indicates that triplet $n=3$ states of He have a significant contribution to the dispersion potential. In model D, He ($n=4$) states have been added to expansion basis in excess to the states of model C. There is a marginal decrease (about 3.6%) in the zero-energy elastic cross section of model D over that of model C. This shows that the scattering parameters presented here (model D) are nearly convergent with respect to the addition of states of the colliding atom. It is evident from Fig. 3 that the s-wave elastic cross sections for the triplet metastable target of all four models are almost equal to each other for incident energies greater than 10^{-6} a.u.

B. $\bar{H}(1s)+He(2\,^1S)$ system

Due to the appreciably long lifetime of the lowest metastable triplet helium state, a lot of different experiments have been performed on this state. On the other hand, $n=2S$ singlet metastable states have less practical importance, although a few experiments have also been executed on this atomic state. Presently $He(2\,^1S)$ has been reported to have appreciable abundance compared to $He(1\,^1S)$, which has been utilized in Penning plasma diagnoses [22]. Here we present the results of a pseudostate close-coupling calculation for the $\bar{H}(1s)+He(2\,^1S)$ system, using all the models employed in the case of the triplet target. The metastable singlet target differers from the triplet target due to the presence of the deexcitation channel, which may lead to Penning ionization. We have performed the calculations for the present system using the following two basis sets: $\bar{H}(1s)+He(2\,^1S)$ and $\bar{H}(1s)+He(1\,^1S,2\,^1S)$. The elastic results of both the calculations are almost identical and the probability of deexcitation of He to its ground state is found to be negligible. Guided by this finding, we have neglected the ground state of the target. This allows us to treat the two metastable species on equal footing. From the academic point of view, the investigation of interaction dynamics in this system and comparison with the corresponding triplet case are of importance as the dispersion coefficients for the interaction for $H(1s)+He(2\,^1S)$ system are greater than the corresponding values for $H(1s)+He(2\,^3S)$ system (see Table I). That is, for the singlet He target the long-range interaction will be more attractive than that for the triplet target.

Table III compares the s-wave elastic phase shifts for the $\bar{H}(1s)+He(2\,^1S)$ system using all four PSCCA models [34]. The phase shifts of models A and B are almost identical, showing once again that the two pseudostate descriptions of the antihydrogen atom are nearly equivalent. The very low-energy cross sections of models A and B differ by less than 0.4%. As in the case of the triplet target, here also the $n=3$ states (singlet) of the helium atom have considerable effect on the elastic channel. The cross section of model C is even

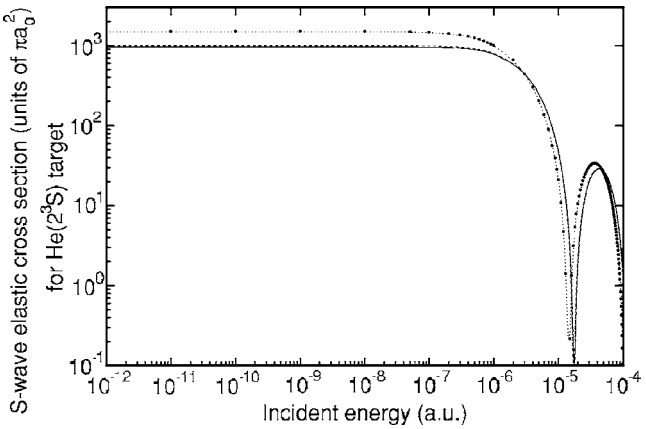

FIG. 3. s-wave elastic cross section (in units of πa_0^2) for $\bar{H}(1s)+He(2\,^3S)$ scattering. Curves: circles, model A; dotted, model B; dashed, model C; solid, model D.

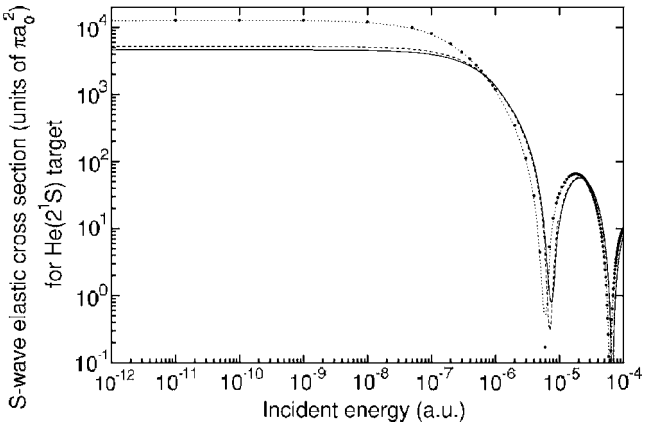

FIG. 4. s-wave elastic cross section (in units of πa_0^2) for $\bar{H}(1s)+He(2\,^1S)$ scattering. Curves: circles, model A; dotted, model B; dashed, model C; solid, model D.

less than half the value obtained in model A. This is nothing but the manifestation of the dominance of the van der Waals interaction of the system. The inclusion of $n=4$ states of the target atom in model D results in a decrease in the cross section by about 13% from the result of model C. This decrease is about 3.6% for the triplet target. This shows that even $n=4$ singlet states are very important in determining the elastic scattering parameters. In other words, a comparison of the results of the two systems shows that the effect of the long-range forces is more important for the singlet metastable He than for the triplet. One of the reasons for the discrepancy of the convergence of the scattering parameters of the systems may be due to the neglect of the stable ground state in the case of the singlet metastable target. However, our test calculations with simple basis sets show that the inclusion of the deexcitation channel has hardly any effect on the elastic channel. As for the triplet target, here also all the four models predict nearly equal values (Fig. 4) for the elastic cross section for energy greater than 10^{-6} a.u. The low-energy elastic cross section for the metastable singlet target is greater than the corresponding values for the triplet target.

C. Scattering lengths

We have performed calculations down to 10^{-16} a.u. for both the systems and calculated the scattering lengths using effective range theory. We have used the values of phase shifts in the energy range 10^{-16} to 10^{-8} a.u. In this range the s-wave cross sections for both the systems obey Wigner's threshold law, i.e., cross sections are independent of incident energy. The scattering length is a measure of the cross section for a system with zero relative velocity between the colliding atoms. A knowledge of the scattering length also provides the values for the phase shifts in Wingner's region, i.e., in the region of constancy of the cross section. Table IV displays the scattering lengths for the systems using all four PSCCA models. It is found that the scattering length for the triplet target is almost convergent with respect to the addition of the atomic states in the basis set, while for singlet helium there is scope to improve the results by adding still higher ($n>4$) states of the target atom. However, the present trend shows that the improvement will not be significant.

TABLE IV. s-wave scattering length (in a.u.) for both systems.

System	Model A	Model B	Model C	Model D
$\bar{H}(1s)+He(2\,^3S)$	19.44	19.54	15.80	15.51
$\bar{H}(1s)+He(2\,^1S)$	56.19	56.08	36.45	34.02

The values of the scattering parameters are mostly governed by the asymptotic nature of the interaction potential. A comparison of the dispersion coefficients (Table I) shows that the asymptotic potential for the singlet helium target is more attractive than the triplet one. That is, the deformations (arising from dipole and higher-order moments) of the metastable helium targets are greater for the singlet state than for the triplet one. This fact has been well manifested in our CCA calculations; the s-wave elastic scattering length for the collision of ground-state antihydrogen with metastable singlet helium is much greater than the corresponding value for the triplet target.

A comparison of the result of model A with those of model C and D show that the asymptotic potentials of order higher than R^{-6} have considerable effect on the thermal energy elastic scattering. In view of the variation of the scattering length with the co-efficient of the asymptotic potential [38], it is evident that the short-range interaction also influences the low-energy scattering to some extent. Thus, in cold atomic collisions, the value of the scattering length is very sensitive to the details of the interaction potential. The systematic improvement of our present scattering length for each system shows that the potential generated dynamically within the CCA gets refined consistently with the enlargement of the basis set.

D. Cooling of $\bar{H}(1s)$

The rate of cooling of $\bar{H}(1s)$ through evaporation in a buffer gas depends on the values of the elastic cross section of the antiatom with the buffer gas. The zero-energy cross sections for the scattering of $\bar{H}(1s)$ off metastable helium atoms are much greater than the corresponding values for $H(1s)$ and $He(1\,^1S)$ targets. From that point of view, the metastable He may be considered to be an efficient candidate as buffer gas. Furthermore, the small mass of He compared to other targets (except hydrogen and its isotopes) will result in small transfer of momentum by the buffer gas to the antiatom. One defines the efficiency of cooling $\bar{H}$, taking H as reference, as $f=\frac{M_{\bar{H}}}{M_A}\frac{\sigma_{A\text{-}\bar{H}}}{\sigma_{H\text{-}\bar{H}}}$. Table V compares the efficiency of evaporative cooling of the ground-state antiatom in different atomic buffer gases. It is found that for the metastable helium targets the elastic cross sections at thermal energies are much greater than that for the ground-state target. Such a feature of the elastic cross section has also been noticed for electron impact scattering off different helium states [18]. Since the rate of evaporative cooling is directly proportional to the elastic cross section, antihydrogen may be cooled ef-

TABLE V. Comparison of efficiency of cooling, f, of $\bar{H}(1s)$ by different atomic buffer gases.

Target	Scattering length (a.u.)	Efficiency
$^1H(1s)$ [39,40]	8.19	1
$^4He(1\ ^1S)$ [12]	2.71	0.11
$^4He(2\ ^1S)$	34.02	4.31
$^4He(2\ ^3S)$	15.51	0.90
$^7Li(2s)$ [16]	48.49	5.01

ficiently in the $n=2$ metastable helium buffer gases than ground-state helium buffer gas.

V. CONCLUSION

The present study reports the s-wave scattering parameters (phase shift, scattering length and cross section) for $\bar{H}$ interacting with metastable atomic heliums $He(2\ ^1S)$ and $He(2\ ^3S)$ targets in the energy range 10^{-16} to 10^{-4} a.u. A nonadiabatic, quantal coupled-state model has been used to investigate the systems. The total wave function of the system has been expanded in terms of the orbitals describing the bound states of the individual atoms. All the short- and long-range potentials can be generated dynamically in the calculation. The present CCA models include the long-range potential properly as is evident from Table I. Since for both the systems under consideration the interaction potentials (both long and short range) are of importance, the projectile atom has been described in two different pseudostate bases (PSCCA). It has been found that the two sets of pseudostates used to describe antihydrogen atoms for both systems predict nearly the same results for the elastic scattering parameters. We have included up to $n=4$ states of the target He atom in the expansion basis. With the extension of the basis set, the present scattering lengths for both the systems get improved unambiguously, which stands in favor of the consistency of our calculation. Our results for the metastable triplet target, i.e., $He(2\ ^3S)$, are more accurate than those for the singlet target. The low-energy elastic cross sections for antihydrogen scattering of the lowest metastable singlet and triplet helium targets are approximately 150 and 31 times greater than the corresponding values for the ground-state target.

The present investigation has not considered the effect of rearrangement channels and of the strong interaction on the elastic scattering. The inclusion of these two effects will modify the present results. However, the trend of the results for both systems suggests that present study provides reliable estimates for the s-wave elastic scattering parameters without the effects of strong interaction and rearrangement processes on elastic channel.

ACKNOWLEDGMENTS

The authors acknowledge the financial support of the Department of Science and Technology, Govt. of India (DST Project No. SR/S2/LOP-10/2003).

[1] G. Baur *et al.*, Phys. Lett. B **368**, 251 (1996).
[2] G. Blanford, D. C. Christian, K. Gollwitzer, M. Mandelkern, C. T. Munger, J. Schultz, and G. Zioulas, Phys. Rev. Lett. **80**, 3037 (1998).
[3] M. Amoretti *et al.*, Nature (London) **419**, 456 (2002).
[4] G. Gabrielse *et al.*, Phys. Rev. Lett. **89**, 213401 (2002).
[5] N. Madsen *et al.*, Phys. Rev. Lett. **94**, 033403 (2005).
[6] C. H. Storry *et al.*, Phys. Rev. Lett. **93**, 263401 (2004).
[7] Froelich and co-workers have employed an adiabatic molecular expansion technique to estimate elastic and different inelastic probabilities; e.g., P. Froelich, S. Jonsell, A. Saenz, B. Zygelman, and A. Dalgarno, Phys. Rev. Lett. **84**, 4577 (2000); S. Jonsell, A. Saenz, P. Froelich, B. Zygelman, and A. Dalgarno, J. Phys. B **37**, 1195 (2004).
[8] Armour and co-workers have employed the adiabatic molecular expansion technique together with the Kohn variational method; e.g., E. A. G. Armour and C. W. Chamberlain, in *New Directions in Antimatter Chemistry and Physics*, edited by C. M. Surko and F. A. Gianturco (Kluwer Academic Publishers, Dordrecht, 2001); E. A. G. Armour, Y. Lin, and A. Vigier, J. Phys. B **38**, L47 (2005).
[9] Ghosh and co-workers employed the nonababatic atomic orbital expansion technique; e.g., P. K. Sinha and A. S. Ghosh, Europhys. Lett. **49**, 558 (2000); P. K. Sinha, P. Chaudhuri, and A. S. Ghosh, Phys. Rev. A **67**, 052509 (2003).
[10] A. Y. Voronin and J. Carbonell, Nucl. Phys. A **689**, 529 (2001).
[11] K. Strasburger and H. Chojnacki, Phys. Rev. Lett. **88**, 163201 (2002).
[12] P. K. Sinha and A. S. Ghosh, Phys. Rev. A **68**, 022504 (2003).
[13] P. K. Sinha and A. S. Ghosh, Phys. Rev. A **71**, 012505 (2005).
[14] S. Jonsell, P. Froelich, S. Eriksson, and K. Strasburger, Phys. Rev. A **70**, 062708 (2004).
[15] K. Strasburger, H. Chojnacki, and A. Sokolowska, J. Phys. B **38**, 3091 (2005).
[16] P. K. Sinha and A. S. Ghosh, Phys. Rev. A **72**, 052509 (2005).
[17] P. K. Sinha and A. S. Ghosh, Phys. Rev. A **73**, 032711 (2006).
[18] D. C. Cartwright and G. Csanak, Phys. Rev. A **55**, 1962 (1997).
[19] L. J. Uhlmann, R. G. Dall, A. G. Truscott, M. D. Hoogerland, K. G. H. Baldwin, and S. J. Buckman, Phys. Rev. Lett. **94**, 173201 (2005).
[20] F. Pereira Dos Santos, J. Leonard, J. Wang, C. J. Barrelet, F. Perales, E. Rasel, C. S. Unnikrishnan, M. Leduc, and C. Cohen-Tannoudji, Phys. Rev. Lett. **86**, 3459 (2001).
[21] M. Kurahashi, T. Suzuki, and Y. Yamauchi, Appl. Phys. Lett. **85**, 2869 (2004).
[22] P. X. Feng and B. Weiner, J. Phys. B **37**, 3265 (2004).
[23] K. Bhadra, J. Callaway, and R. J. W. Henry, Phys. Rev. A **19**, 1841 (1979).
[24] T. G. Winter and C. C. Lin, Phys. Rev. A **12**, 434 (1975).
[25] T. R. Proctor and W. C. Stwalley, J. Chem. Phys. **68**, 5292

(1978).
[26] R. J. Damburg and E. Karule, Proc. Phys. Soc. London **90**, 637 (1967).
[27] W. C. Fon, K. A. Berrington, P. G. Burke, and A. E. Kingston, J. Phys. B **14**, 1041 (1981).
[28] A. A. Kernoghan, M. T. McAlinden, and H. R. J. Walters, J. Phys. B **28**, 1079 (1995).
[29] C. P. Campbell, M. T. McAlinden, F. G. R. S. MacDonald, and H. R. J. Walters, Phys. Rev. Lett. **80**, 5097 (1998).
[30] S. Gilmore, J. E. Blackwood, and H. R. J. Walters, Nucl. Instrum. Methods Phys. Res. B **221**, 126 (2004).
[31] S. H. Patil and K. T. Tang, J. Chem. Phys. **107**, 3894 (1997).
[32] S. H. Patil and K. T. Tang, J. Chem. Phys. **106**, 2298 (1997).
[33] D. M. Bishop and J. Papin, Int. J. Quantum Chem. **45**, 349 (1993).
[34] The phase shifts of Tables II and III are in the range $\pm\pi/4$, the output of the arctangent in FORTRAN. The change of sign of the phase shifts at energies where the corresponding cross sections are smooth denotes the crossing of values $\pm(2n+1)\pi/2$. To ascertain the actual values of the phase shifts and consequently the number of bound states one needs to perform calculation at very high energies and go on lowering the energy value. But this will require huge computation time.
[35] To get the phase shifts at energy 10^{-6} a.u. one needs to add $\pi/2$ to the corresponding entries of Tables II and III.
[36] It has been observed that there exists at least one bound state for each system. This means that the phase shift approaches π in the zero-energy limit.
[37] Z. C. Yan, J. F. Babb, A. Dalgarno, and G. W. F. Drake, Phys. Rev. A **54**, 2824 (1996).
[38] V. V. Flambaum, G. F. Gribakin, and C. Harabati, Phys. Rev. A **59**, 1998 (1999).
[39] P. K. Sinha, P. Chaudhuri, and A. S. Ghosh, Phys. Rev. A **69**, 014701 (2004).
[40] In Ref. [39] it was quoted that $a_0=7.7$ a.u. There was a slight convergence problem with respect to the quadrature points used. With the extended points, we get the final convergent values as $a_0=8.19$ a.u. compared to the recently reported values in Ref. [41] 8.383 a.u. using an optical potential and 8.414 a.u. using a scattering length approach.
[41] S. Jonsell, A. Seanz, P. Froelich, B. Zygelman, and A. Dalgarono, Can. J. Phys. **83**, 435 (2005)]